Radio Science, Volume 31, Number 5, Pages 1011–1024, September–October 1996

The electrostatic characterization of an n-element planar array using the singularity expansion method

J. E. Mooney, L. S. Riggs, and M. E. Baginski

Department of Electrical Engineering, Auburn University, Auburn, Alabama

Abstract. In this paper, the singularity expansion method (SEM) is used to describe the electrostatic charge distribution on an array of thin linear antennas placed in a uniform electric field. The SEM, which has primarily been used to analyze transient scattering problems, decomposes the electromagnetic interaction process into various quantities such as singularities and modes. Using the SEM, the step plane wave induced transient current on the array is expanded in terms of its singularities (poles) in the Laplace transform (complex frequency domain.) The continuity equation is applied to the induced current expression to obtain the transient charge. The electrostatic charge distribution on the array is found by using the final value theorem on the transient charge expression. It is well known that the SEM factorization of a single linear element reveals that a single pole exists in the fundamental resonance region (near $\omega L/c = \pi$, where L is the length of the scatterer). For a two-element array, two poles are observed in the fundamental resonance region. This trend continues such that an n-element array has n poles in the fundamental resonance region. Associated with each pole is a unique modal current and corresponding charge distribution. For example, one of the two fundamental resonance region poles of the two-element array produces half-wavelength sinusoidal current distributions whose directions are the same on one scatterer but opposite on the other. The remaining fundamental resonance region pole produces half-wavelength sinusoidal current distributions whose directions are the same on both scatterers. Corresponding to each mode is a coupling coefficient which determines how much a particular mode couples into the response. A generalization of these results for an n-element array will be given. Furthermore, the electric polarizability is derived in terms of the SEM electric charge description. The value of this research lies in the elegance and strength of the SEM to factor a problem into various quantities which depend on different variables of the problem. By using the SEM to analyze the n-element planar array, a much deeper comprehension of the fundamental aspects of the electrostatic interaction process is achieved.

1. Introduction

Understanding how the electromagnetic charging of a system affects an electrical system's characteristics is a topic being given increased attention. This is due mainly to the role quasi-static charging may play in the possible degradation of the system's performance. In the specific case of antennas placed on outdoor platforms, the adjacent terrain and the Earth's fair weather electric field dictate how the electrostatic charge will be distributed. By using the singularity expansion method (SEM) described here, a more complete understanding of how the antenna system responds to both electrostatic and time-varying electromagnetic fields can be accomplished. This type of information is valuable to the design engineer in assessing lightning hazards, the possibility of coronal currents, and ground protection schemes [*Uman*, 1969].

The singularity expansion method allows one to treat a conducting body in a manner similar to that

Paper number 96RS01929.
0048-6604/96/96RS-01929$11.00

used in classical circuit theory. In circuit theory, the response of a linear circuit excited by an arbitrary waveform may be determined by knowledge of the location of any singularities of the response function as well as the corresponding residues. In a distributed system (e.g., a conducting body), an infinite number of singularities exist, and associated with each is a natural modal current and charge distribution. For an arbitrary excitation, one need only determine the extent to which each natural mode has been excited. This is determined by the coupling coefficient associated with a given natural mode [*Riggs et al.*, 1989].

The principal advantage of the SEM is its ability to break down the electromagnetic interaction process into meaningful parameters such as poles, modes, and coupling coefficients. Definitions for these SEM parameters will be presented, employing a method of moments approximation to the continuous operator electric field equation (EFIE) in terms of the current induced on the array. The research described here principally focuses on the mathematical development of the SEM that will describe the antenna system's behavior for several cases. The results show very good agreement when compared with the method of moments (MOM) electrostatic analysis. The main intent of this work is to provide a clearer view of the fundamental aspects of electrostatic interaction than is available through conventional analysis methods.

2. Theoretical Development

As a starting point to the SEM discussion, consider the array composed of perfectly conducting thin cylindrical elements, as shown in Figure 1. Impinging on this array is some incident field generated by a distant source. The impinging field induces current and charge on the elements, and these sources in turn radiate a scattered field. Owing to the perfectly conducting nature of the elements, the total tangential electric field on the surface of the conductors must be zero; that is, the tangential component of the incident electric field must exactly cancel the tangential component of the scattered electric field. Utilizing standard potential theory [*Harrington*, 1961], the scattered electric field can be expressed in terms of an integro-differential operation on the induced current. This expression and the boundary conditions result in an electric field integral equation (EFIE) in terms of the unknown surface currents on the the elements [*Pocklington*, 1897].

An approximate solution to the EFIE can be obtained by employing the method of moments [*Harrington*, 1968]. A pulse expansion of the unknown current I and pulse testing of the EFIE yields the familiar network matrix equation for the induced current cast explicitly in terms of s,

$$\overline{V}(s) = \mathbf{Z}(s)\,\bar{I}(s) \tag{1}$$

where $\mathbf{Z}(s)$ is the $N \times N$ system impedance matrix, $\bar{I}(s)$ is the system current response vector of length N, and $\overline{V}(s)$ is the system voltage excitation vector of length N. The solution of (1) can be written in the form

$$\bar{I}(s) = \frac{\operatorname{adj} \mathbf{Z}(s)}{\det \mathbf{Z}(s)}\,\overline{V}(s) \tag{2}$$

where the inverse of $\mathbf{Z}(s)$ has been expressed as

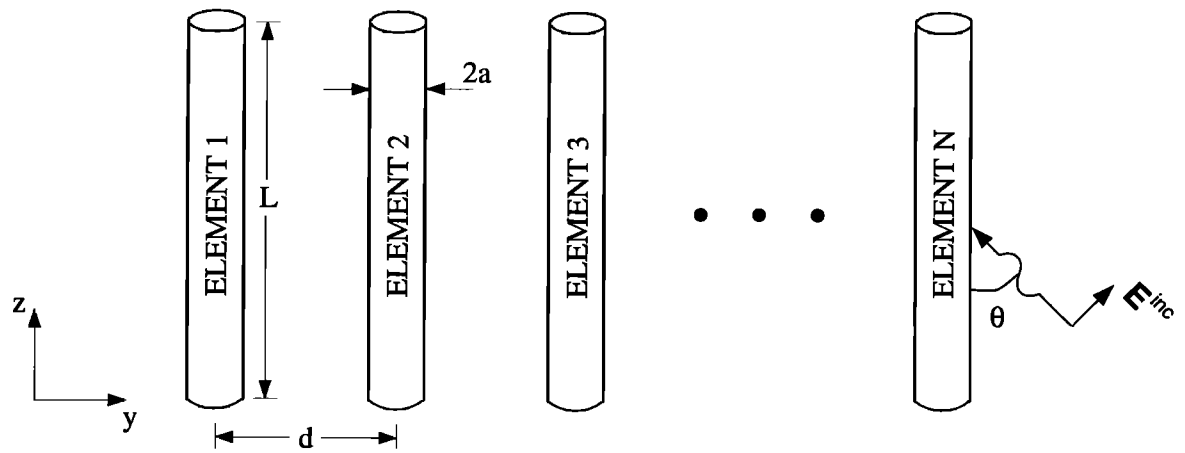

Figure 1. An n-element array.

$$\mathbf{Z}^{-1}(s) = \frac{\text{adj}\,\mathbf{Z}(s)}{\det \mathbf{Z}(s)}. \tag{3}$$

The singularities (poles) of the system are those complex frequencies that force the determinant of $\mathbf{Z}(s)$ to be zero. These singularities, denoted by s_α, are termed natural resonant frequencies since they result in nontrivial solutions to

$$\mathbf{Z}(s_\alpha)\,\bar{I}(s_\alpha) = 0. \tag{4}$$

These frequencies are "natural" in the sense that at these frequencies, the scatterer can have a response without any excitation.

On the basis of the physical nature of the scatterer, several conclusions can be deduced regarding the location of the natural resonances in the complex plane. To ensure the scatterer has a decaying response, the poles must lie in the left half plane. Furthermore, except for those located on the negative real axis, the poles must occur in conjugate pairs to guarantee a real time domain response. Finally, no poles can lie on the $j\omega$ axis because the body is losing energy through radiation.

When the poles and corresponding residues are known, the inverse of the system impedance matrix $\mathbf{Z}^{-1}(s)$ can be expanded in a singularity series [*Boas*, 1987], hence the acronym SEM. By performing such an expansion, $\mathbf{Z}^{-1}(s)$ can be written as

$$\mathbf{Z}^{-1}(s) = \sum_\alpha \frac{\mathbf{R}_\alpha}{s - s_\alpha} + \text{possible entire function} \tag{5}$$

where $\mathbf{R}_\alpha$ is the residue matrix associated with the αth singularity. Note that in the expansion, the singularities are assumed to be poles of the first order. This assumption is valid for perfectly conducting spheres and thin cylindrical wires [*Baum*, 1971], and it has been substantiated numerically. The inclusion of the entire function is required for convergence of the series [*Baum*, 1976]. Without the entire function, the expansion cannot represent any essential singularities that may exist at infinity in the complex plane. Since the elements of $\mathbf{Z}^{-1}(s)$ are of the form $e^{s\tau}$, singular behavior may occur as $s \to \infty$ [*Tesche*, 1973]. However, for the types of objects considered here, the inclusion of the entire function is not necessary.

The next step in the formulation of the SEM description of the transient current is to calculate the residues. The residue matrix $\mathbf{R}_\alpha$ at s_α can be evaluated via the Cauchy residue theorem

$$\mathbf{R}_\alpha = \frac{1}{2\pi j}\int_{c_\alpha} \mathbf{Z}^{-1}(s)\,ds \tag{6}$$

where c_α denotes a contour enclosing the pole at $s = s_\alpha$. It has been shown by Baum [1971] and others that $\mathbf{R}_\alpha$ is dyadic; that is, its elements can be calculated as the outer product of elements taken from two column vectors. In addition to being dyadic, $\mathbf{R}_\alpha$ is symmetric because the EFIE was used in the initial formulation [*Riggs*, 1985]. As a result, the row and column vectors of $\mathbf{R}_\alpha$ are identical. Exploiting the dyadic and symmetric properties, $\mathbf{R}_\alpha$ can be written as

$$\mathbf{R}_\alpha = \beta_\alpha \overline{M}_\alpha \overline{M}_\alpha^T \tag{7}$$

where $\overline{M}_\alpha$ is the αth natural modal current distribution, and the superscript 'T' denotes the matrix transpose operation. The parameter β_α is a complex proportionality constant which is chosen so that the maximum value of $\overline{M}_\alpha$ is real and unity.

Using the factored form of $\mathbf{R}_\alpha$ in (2), the expression for the induced current becomes

$$\bar{I}(s) = \sum_\alpha \frac{\beta_\alpha \overline{M}_\alpha \overline{M}_\alpha^T}{s - s_\alpha}\overline{V}(s). \tag{8}$$

The voltage excitation vector $\overline{V}(s)$ can be written more specifically as

$$\overline{V}(s) = f(s)\,\overline{\Lambda}(s) \tag{9}$$

where $f(s)$ is the functional form of the system excitation vector (impulse, step, ...), and $\overline{\Lambda}(s)$ is the geometry dependent impulsive excitation vector. If plane wave excitation is assumed, then the elements of $\overline{\Lambda}(s)$ are of the form $b \exp\left(-s\frac{\hat{n}\cdot\bar{r}}{c}\right)$, where b is proportional to the component of the incident electric field along the body, $\hat{n}$ is a unit vector in the direction of propagation, and $\bar{r}$ is a position vector.

Using (9) in (8) yields

$$\bar{I}(s) = \sum_\alpha f(s)\frac{\beta_\alpha \overline{M}_\alpha \overline{M}_\alpha^T}{s - s_\alpha}\overline{\Lambda}(s). \tag{10}$$

The SEM parameter known as the coupling coefficient appears in (10) and is defined as

$$\eta_\alpha(s) = \beta_\alpha \overline{M}_\alpha^T \overline{\Lambda}(s). \tag{11}$$

This parameter, which is dependent on the geometry of the scatterer as well as the polarization and propagation direction of the incident wave, governs how much the αth pole-mode pair couples into the response. Substituting (11) into (10), the current response vector becomes

$$\bar{I}(s) = \sum_\alpha f(s)\,\eta_\alpha(s)\frac{\overline{M}_\alpha}{s - s_\alpha}. \tag{12}$$

To obtain an expression for the charge, the continuity equation is employed:

$$\overline{\rho}(s) = -\frac{1}{s}\nabla \cdot \overline{I}(s). \tag{13}$$

Combining the continuity equation with (12), the expression for the charge becomes

$$\overline{\rho}(s) = -f(s)\sum_{\alpha}\eta_{\alpha}(s)\frac{\overline{D}_{\alpha}}{s(s-s_{\alpha})} = f(s)\overline{\Gamma}(s) \tag{14}$$

where $\overline{\Gamma}(s)$ is the "network" impulse charge response and

$$\overline{D}_{\alpha} = \nabla \cdot \overline{M}_{\alpha} \tag{15}$$

defines the αth natural charge mode [*Riggs et al.*, 1989]. Through a partial-fraction expansion of the $[s(s-s_{\alpha})]^{-1}$ term, the expression for the induced charge can be written as

$$\overline{\rho}(s) = -f(s)\left[\sum_{\alpha}\eta_{\alpha}(s)\frac{\overline{D}_{\alpha}}{ss_{\alpha}} - \sum_{\alpha}\eta_{\alpha}(s)\frac{\overline{D}_{\alpha}}{s_{\alpha}(s-s_{\alpha})}\right]. \tag{16}$$

The first term of (16) can be neglected since there is no singularity at $s = 0$ in the complex plane [*Baum*, 1971].

In order to determine the electrostatic charge distribution, an appropriate excitation function $f(s)$ must be chosen so that the array is immersed in a uniform electric field. Although many different excitation functions would result in the same final charge distribution, a simple step excitation will be used here. Thus, substituting s^{-1} in for $f(s)$ and neglecting the first term, (16) becomes

$$\overline{\rho}(s) = \sum_{\alpha}\eta_{\alpha}(s)\frac{\overline{D}_{\alpha}}{s_{\alpha}s(s-s_{\alpha})}. \tag{17}$$

Again, expanding the $[s(s-s_{\alpha})]^{-1}$ term of (17) in partial fractions yields

$$\overline{\rho}(s) = \sum_{\alpha}\eta_{\alpha}(s)\frac{\overline{D}_{\alpha}}{ss_{\alpha}^2} - \sum_{\alpha}\eta_{\alpha}(s)\frac{\overline{D}_{\alpha}}{s_{\alpha}^2(s-s_{\alpha})}. \tag{18}$$

Applying the final value theorem to obtain the electrostatic charge distribution results in

$$\overline{\rho}(t=\infty) = \sum_{\alpha}\eta_{\alpha}(0)\frac{\overline{D}_{\alpha}}{s_{\alpha}^2}. \tag{19}$$

Using (19), the electric polarizability can be expressed in terms of the SEM parameters. If an uncharged conducting body is placed in a uniform electric field, then the resulting net dipole moment $\mathbf{p}$ is given by

$$\mathbf{p} = \oint_S \mathbf{r}\rho(x,y,z)ds \tag{20}$$

where $\mathbf{r} = x\hat{a}_x + y\hat{a}_y + z\hat{a}_z$ is the radius vector from the origin to a point on the surface S of the conductor, and $\rho(x,y,z)$ is the surface charge density on S [*Harrington*, 1968]. When thin cylindrical bodies are considered, (20) reduces to a line integral. Using the SEM description for the charge in (19), the surface integral can be approximated as

$$\mathbf{p} = \sum_{n=1}^{N}\Delta\mathbf{r}_n\sum_{\alpha}\eta_{\alpha}(0)\frac{(\overline{D}_{\alpha})_n}{s_{\alpha}^2} \tag{21}$$

where N represents the number of equal length numerical segments on the thin cylinder, Δ is the length of each segment, and $\mathbf{r}_n$ is the radius vector from the origin to the center of the nth segment. The quantity $(\overline{D}_{\alpha})_n$ is the value of the αth charge mode on the nth segment. The dipole moment is proportional to the impressed field $\mathbf{E}^i$ which produces the charge $\rho(x,y,z)$; therefore a polarizability tensor $[\mathbf{X}]$ may be defined as

$$\mathbf{p} = \begin{bmatrix} \chi_{xx} & \chi_{xy} & \chi_{xz} \\ \chi_{yx} & \chi_{yy} & \chi_{yz} \\ \chi_{zx} & \chi_{zy} & \chi_{zz} \end{bmatrix}\begin{bmatrix} E_x^i \\ E_y^i \\ E_z^i \end{bmatrix} = [\mathbf{X}]\cdot\mathbf{E}^i \tag{22}$$

To find a particular element of $[X]$, say, χ_{xy}, $p_x = \chi_{xy}$ is found for an applied field $(E_x^i, E_y^i, E_z^i) = (0,1,0)$.

3. Numerical Results

In this section, the electrostatic characterization of two-, three-, four-, and five-element arrays will be given. The elements of the planar arrays under consideration each have a commonly used radius-to-length ratio, a/L, of 0.005. For the two- and three-element arrays, two cases will be presented where the separation distance-to-length ratio, d/L, is 0.10 and 1.0. The results for the four- and five-element arrays will be limited to the case where d/L is 0.10. The radius a and the separation distance d parameters are illustrated in Figure 1. The electrostatic charge distribution on these arrays using the SEM

will be compared with the direct MOM solution for the same obtained from the electrostatic scalar potential equation. In addition to presenting the electrostatic charge distribution and electric polarizability, a discussion of some relationships among the the SEM parameters of the n-element arrays will be given.

Before presenting the results for the two-, three-, four-, and five-element arrays, it is interesting to give a brief discussion of the SEM parameters associated with a single linear conductor. An SEM characterization of a single linear element reveals that the poles of this object occur in layers roughly parallel to the $j\omega$ axis. To distinguish among the poles in the s plane, they are labeled with two indices, $s_{l,n}$, where l denotes the layer and n refers to the poles in that layer. The poles in the fundamental layer, $l = 1$, reside very close to the $j\omega$ axis. Only these poles contribute significantly to the response of the scatterer, since their nearness to the $j\omega$ axis implies a small damping constant. Thus the poles with a large real part (Ω), such as those in the second layer, are normally not considered, since their effects are negligible due to large damping constants. The imaginary parts of the fundamental layer poles, when multiplied by the length of the wire L and divided by the speed of light c, occur at approximately $k\pi$, where k is an integer. The first pole of the first layer, s_{11}, lies near $\omega L/c = \pi$. Singularities residing in this general vicinity are termed fundamental resonance region poles. Subsequent poles in the first-layer are harmonics of the fundamental and have imaginary parts near 2π (s_{12}), 3π (s_{13}), etc. Another way to view the location of the first-layer poles is to note that the imaginary parts occur at frequencies where the length of the object is an integer multiple of a half wavelength. This relationship is shown as follows:

$$\frac{\omega L}{c} = k\pi \Rightarrow \frac{2\pi L}{\lambda} = k\pi \Rightarrow L = k\frac{\lambda}{2} \tag{23}$$

where λ is the free space wavelength.

As was mentioned previously, associated with each pole is a unique modal current distribution. The modes for poles lying in the first layer have quasi-sinusoidal current distributions along the length of each element. The fundamental resonance region pole is observed to have a quasi-half-wavelength sinusoidal current distribution, as would be expected from (23). Similarly, second harmonic poles have a full wave quasi-sinusoidal current distribution. Although (23) describes the nature of the distribution for a given harmonic, what is not so obvious is the direction of the current flow on the array associated with a given mode. Examining the location of the poles and the characteristics of their corresponding modal current distributions reveals much about the fundamental electromagnetic interaction process.

Having briefly summarized the SEM parameters for the single element, the pole-mode relationships for the two-, three-, four-, and five-element arrays

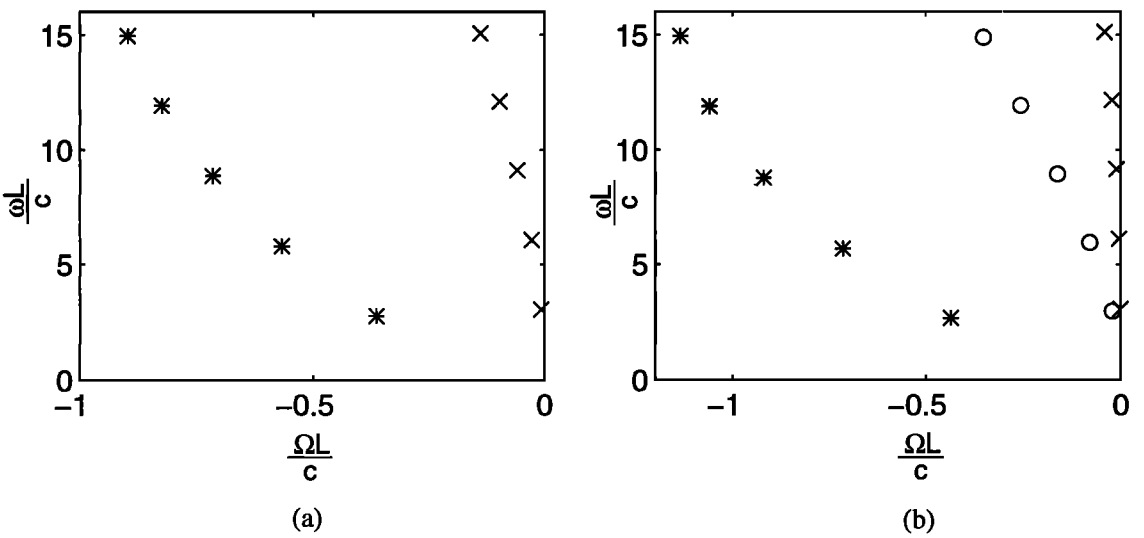

Figure 2. The pole positions for the first five harmonics of the (a) two-element array and (b) three-element array.

can now be discussed. The SEM factorization of the two-element array reveals that two poles reside in the general location of the complex plane where the isolated element has a single pole. Thus, in the fundamental resonance region, the two-element array has two poles. Furthermore, two poles exist in each of the higher-order harmonic regions as well. Figure 2a illustrates the pole positions for the first five harmonics of the two-element array. As one might anticipate, the three-element array has three poles in the complex plane where the single element has only one. The pole positions for the three-element array are shown in Figure 2b. This trend continues as more elements are added to the array such that an n-element array has n poles in the region where the isolated element only has one.

The addition of a singularity for each element added to the array provides for some interesting pole-mode relationships. The two poles for the two-element array can be identified as either a radiation pole or a transmission line pole, depending on the directions of the modal currents which flow on the elements of the arrays. The radiation pole, designated with the asterisk in Figure 2a, has modal currents that flow in the same direction on both elements. This pole, which is located farthest from the $j\omega$ axis, is low Q (defined as the ratio of stored energy to dissipated energy) [*Van Valkenburg*, 1964]; therefore any energy that is coupled into this mode will be rapidly radiated into space. In contrast, the transmission line pole has modal currents that flow in opposite directions. In accordance with Kirchhoff's current law, a symmetric two-wire array with 1 A flowing on one element must have 1 A flowing in the opposite direction on the other element. The transmission line pole, designated with crosses, is located very close to the $j\omega$ axis and therefore is high Q (low damping constant). The real part of the modal current distributions associated with the fundamental radiation and transmission line poles are shown in Figure 3. The imaginary part of the modal current is not shown since it is very small relative to the real part. The imaginary component of the modal current is a result of the wire having a finite diameter. In the limit as the diameter of the wire goes to zero, the modal current will become purely a real quantity.

The three-element array, as previously mentioned, has three poles in the area where the isolated element has only one. By inspecting Figure 2b, one can observe the positions of these singularities. The three-element array also has a radiation pole and a transmission line pole, designated by the asterisks and crosses, respectively. These poles have the same characteristics of the radiation and transmission line poles of the two-element array. Of the pole trio, the radiation pole resides farthest from the $j\omega$ axis and the transmission line pole lies closest. The radiation pole has modal currents that flow in the same direction on all three elements. Furthermore, it has the highest damping (lowest Q) of the three poles. The transmission line pole has modal currents of 0.5 A (amplitude) flowing in the same direction on the outer wires and 1 A flowing in the opposite direction on the center element, which again satisfies Kirch-

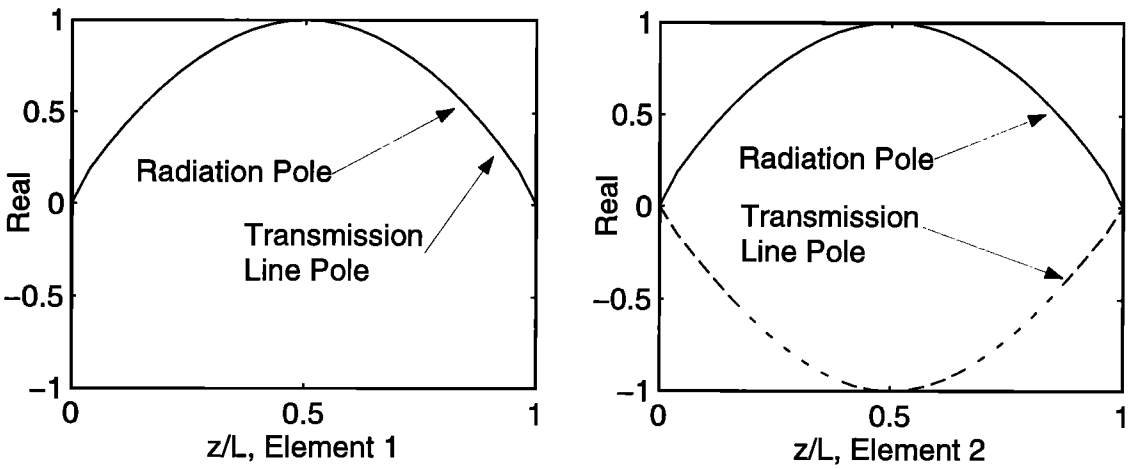

Figure 3. The real modal current distributions for the the fundamental radiation and transmission line poles of the two-element array.

hoff's current law. Because of its close proximity to the $j\omega$ axis, the transmission line pole has a small damping constant and therefore a high Q. The remaining pole is referred to here as the zero-mode pole. As its name suggests, the zero-mode pole has no current on the center element. In Figure 2b, this pole is designated by open circles. The real parts of the modal current distributions of the the fundamental radiation, transmission line, and zero-mode poles of the three-element array are shown in Figure 4. It should be noted that the poles of the arrays are system poles; that is, a pole does not correspond to any particular element of the array but rather to the entire array.

The four- and five-element arrays possess some of the modes of the two- and three-element arrays as well as having some unique modes of their own. As expected, the four-element array has four poles in a given harmonic region, which means it has four distinct modal distributions. Two of these poles are the familiar radiation and transmission line poles. These poles have the same characteristic modal current distributions as discussed previously. The radiation pole has modal currents flowing in the same direction on each element, and relative to the positions of the other three poles, it is located farthest from the $j\omega$ axis. An inspection of the modal current distribution for the transmission line pole reveals 1 A flowing in opposing directions on the inner two elements and 0.5 A flowing in opposing directions on the outer elements. The other two distinct modal current distributions of the four-element array are

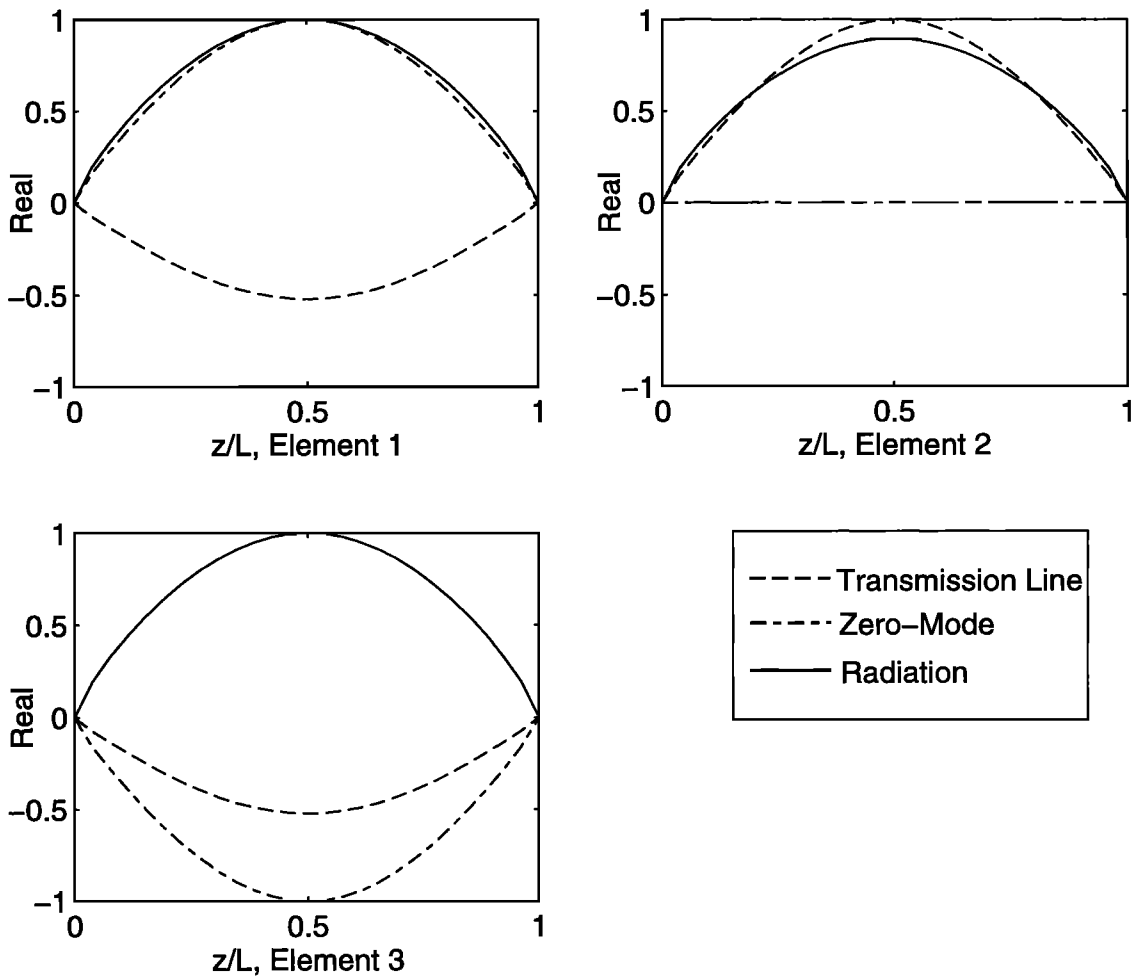

Figure 4. The real modal current distributions for the fundamental radiation, transmission line, and zero-mode poles of the three-element array.

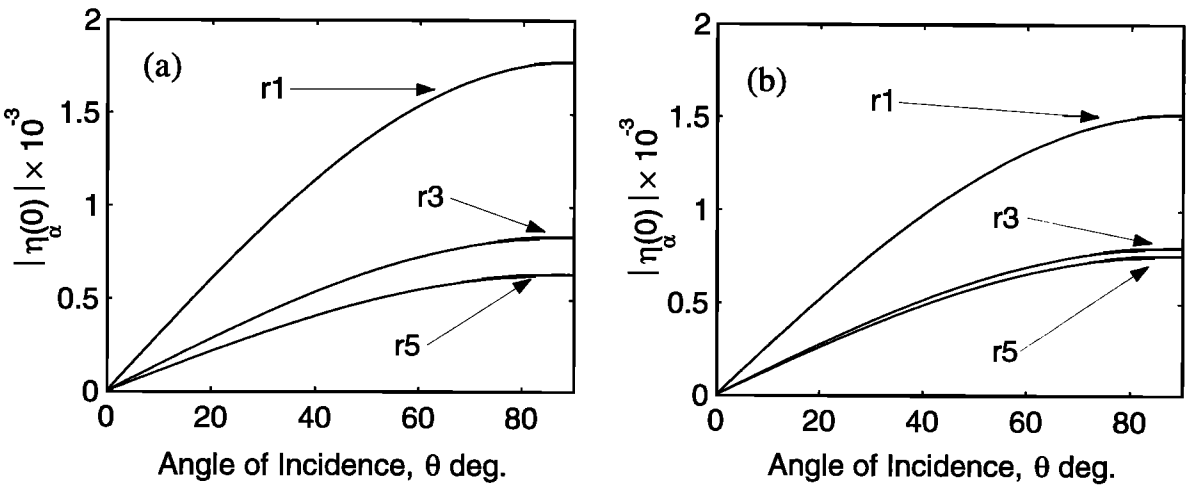

Figure 5. The magnitude of the normalized electrostatic coupling coefficients for the (a) two-element and (b) three-element arrays. The number following the r represents the harmonic of the radiation pole.

interesting, but a physical interpretation requires a more in-depth consideration of the information. The current distributions of these modes are oriented such that the net current flowing over all four elements is zero.

As one would expect, the five-element array has five distinct modes. Three of these are associated with the three-element array. Thus, in addition to two more singularities, the five-element array has a radiation pole, a transmission line pole, and a zero-mode pole. These three poles have the same characteristic modal distributions described earlier for the three-element array. A physical interpretation of the modes of the remaining two singularities is difficult. One significant feature of these modes is that their distributions, when summed over all five elements, is approximately zero.

As was mentioned in the previous section, the coupling coefficient governs how much of each mode couples into the response. The electrostatic coupling coefficient for the two- and three-element arrays as a function of the angle of incidence θ is shown in

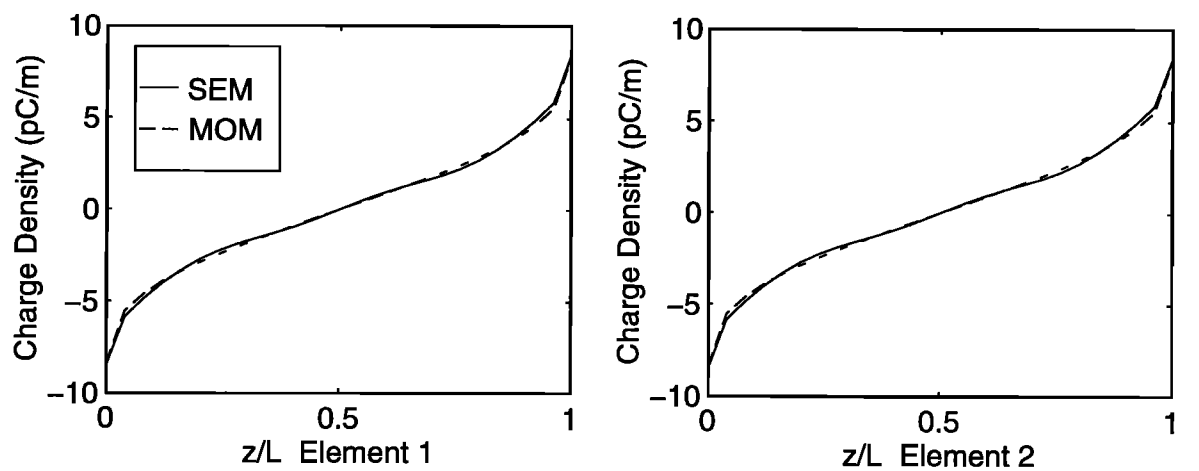

Figure 6. The electrostatic charge distribution for the two-element array $d/L = 0.10$, $a/L = 0.005$. The applied electrostatic field is oriented in the positive z direction ($\theta = 90°$).

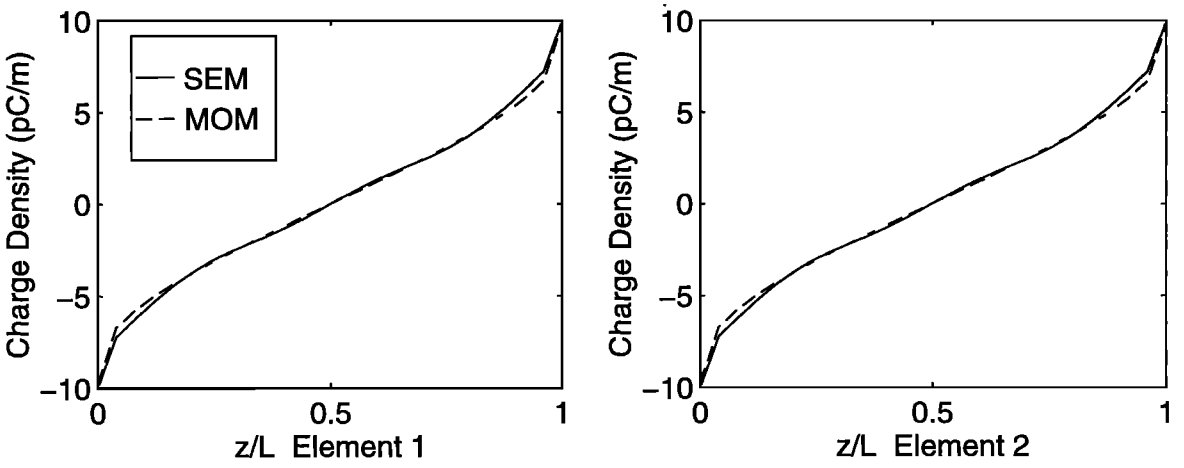

Figure 7. The electrostatic charge distribution for the two-element array $d/L = 1.0$, $a/L = 0.005$. The applied electrostatic field is oriented in the positive z direction ($\theta = 90°$).

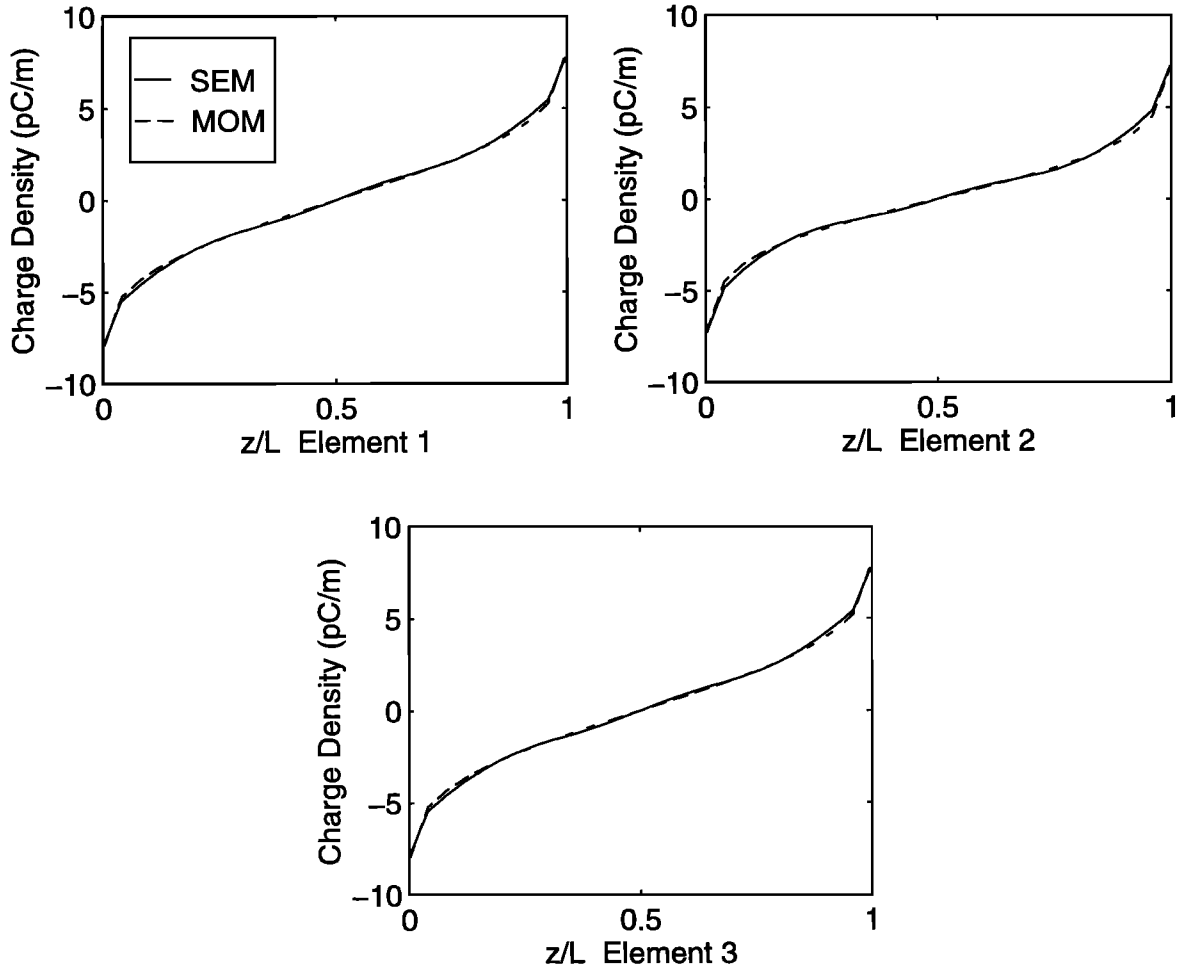

Figure 8. The electrostatic charge distribution for the three-element array $d/L = 0.1$, $a/L = 0.005$. The applied electrostatic field is oriented in the positive z direction ($\theta = 90°$).

Figure 5. The angle of incidence and polarization of the incident electric field is defined in Figure 1. By observing Figures 5a and 5b, one can see that only the odd harmonics of the radiation pole couple significantly into the response. Furthermore, the amount each radiation pole couples into the response decreases with an increase in the order of the harmonic. No mode significantly couples into the response beyond the seventh harmonic. The strong coupling aspect of the radiation pole is due to the fact that its modal currents flow in the same direction on all the elements. None of the modes of the even harmonics couple into the response owing to their distributions having odd symmetry about the center of each element and the excitation being an even function. Furthermore, except for the radiation pole, the modes of all the other singularities are oriented such that they effectively cancel one another. As an example, observe the modal current distribution associated with the zero-mode pole of the three-element array in Figure 4. It is obvious that the currents on the outer elements cancel each other, and the current on the center is already zero. A similar observation can be made about the transmission line mode.

The electrostatic charge distributions for the two-, three-, four-, and five-element arrays are shown in Figures 6 through 11. The electrostatic responses were calculated using a unit step plane wave polarized in the positive z direction ($\theta = 90°$). Only the fundamental, third, and fifth harmonics were used in computing the responses. The SEM electrostatic re-

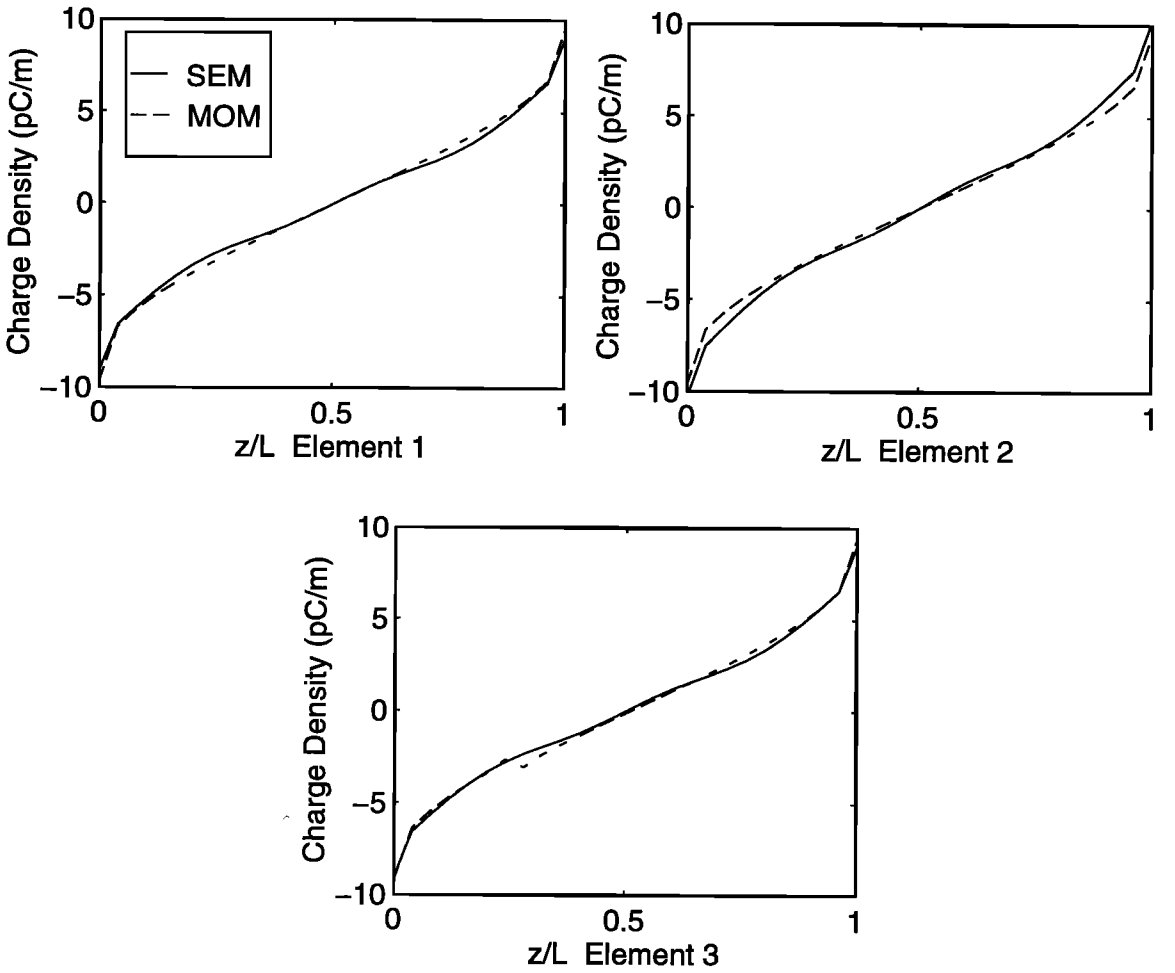

Figure 9. The electrostatic charge distribution for the three-element array $d/L = 1.0$, $a/L = 0.005$. The applied electrostatic field is oriented in the positive z direction ($\theta = 90°$).

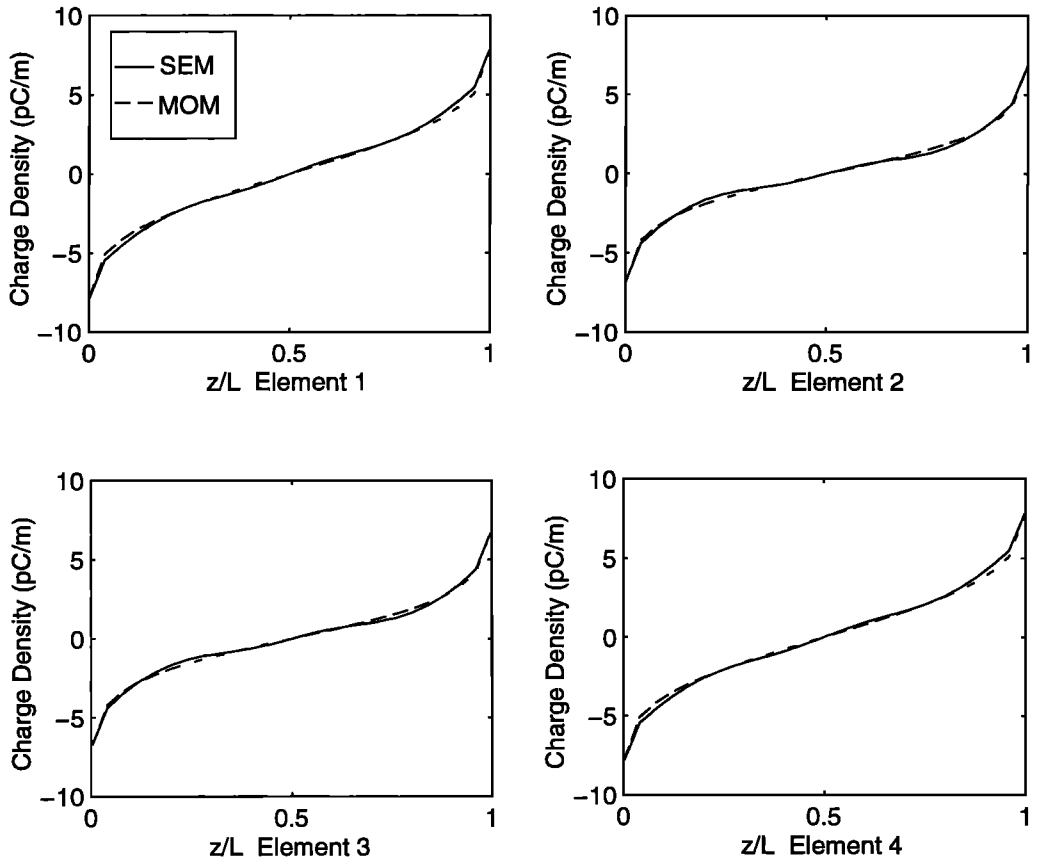

Figure 10. The electrostatic charge distribution for the four-element array $d/L = 0.10$, $a/L = 0.005$. The applied electrostatic field is oriented in the positive z direction ($\theta = 90°$).

sponses are compared with the direct MOM solution of the electrostatic scalar potential equation. From the results, it is obvious that the SEM agrees well with the direct MOM solution in all cases.

The electric polarizability for the two-, three-, four-, and five-element arrays is shown in Table 1. The values shown in this table represent the χ_{zz} element of the polarizability tensor $[X]$, since the electrostatic responses were calculated using an electric field polarized in the positive z direction. It is interesting to note that the polarizability increases with the number of elements in the array. This trend can be explained by noting that the effective surface area of the system increases as elements are added. Also shown in Table 1 is the polarizability χ_{zz} for the two- and three-element arrays with varying distance-to-length ratios. There seems to be an increase in χ_{zz} as d/L is increased. Future work in this area will consider if this trend continues as d/L is increased.

4. Practical Applications

Prior to listing some of the possible applications that the SEM technique could be used for, it is important to underscore the fundamental reason that SEM lends itself to the design phase of the system (an n-element array in this case). The SEM analysis allows the user to extract information about the specific behavior of the entire system for any electrical stimuli by virtue of the "pole constellation plot." This pole constellation plot parallels the transfer function (usually designated H(s)) for a linear system's input/output relationship. In the case considered here, this specifically allows the system's behavior to be easily predicted for any given electrical excitation.

Assuming the array beam pattern, spacing, and electrical feed specifications are known, one of the next features that should be characterized is the sys-

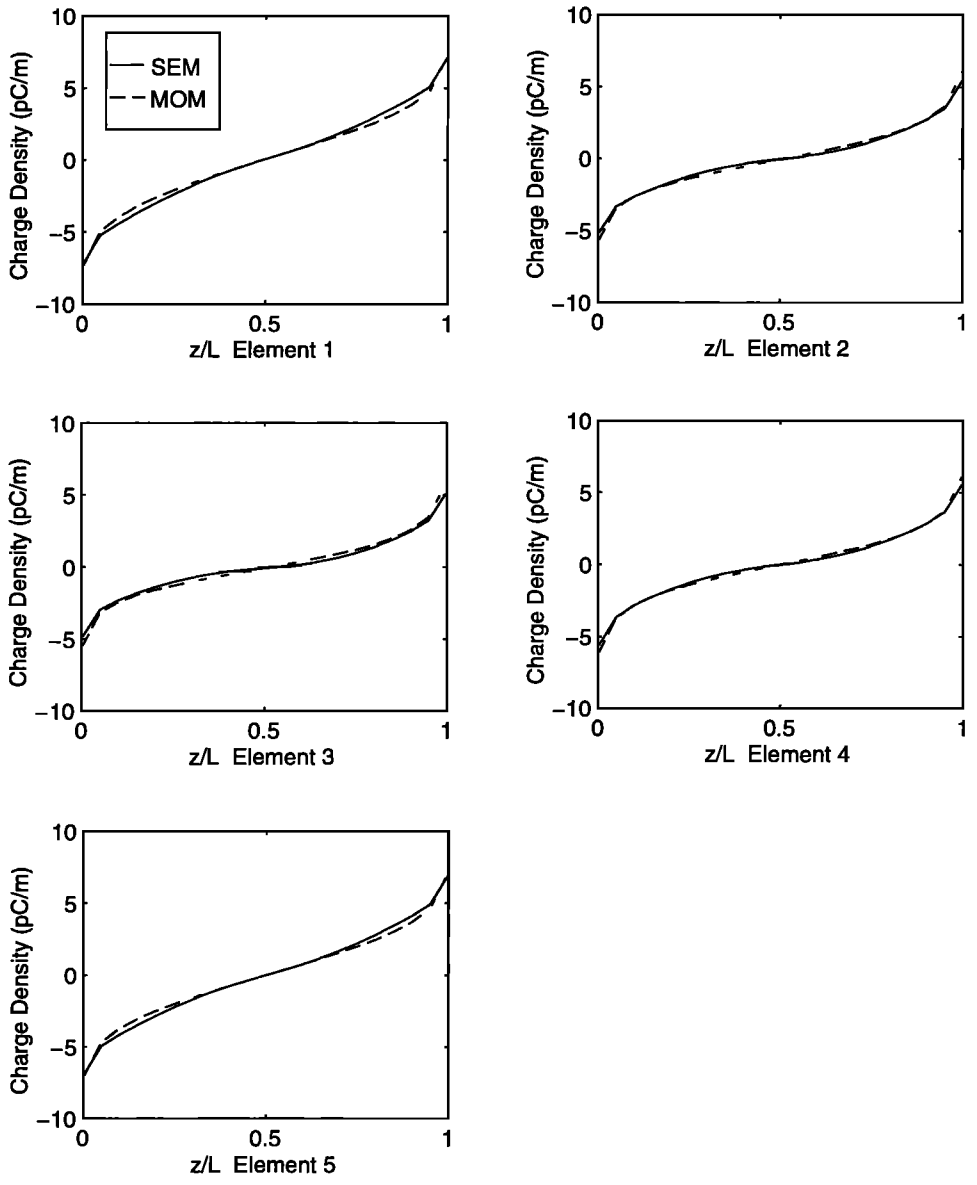

Figure 11. The electrostatic charge distribution for the five-element array $d/L = 0.10$, $a/L = 0.005$. The applied electrostatic field is oriented in the positive z direction ($\theta = 90°$).

tem's overall response to lightning. This can be done in a straightforward manner either by convolution of the time domain lightning current signature at the point of attachment with system time domain transfer function (usually designated $h(t)$) or by multiplication of the lightning current signature's Laplace transform and the system's transfer function ($H(s)$) previously discussed.

In contrast, to obtain a transient result from a frequency domain MOM approach, the matrix equation in (1) must be solved over a wide range of frequencies. The frequency domain data generated from this repetitive process is then inverse Fourier transformed to produce the desired time domain result. Although the inverse Fourier transform can be computationally intensive, its computation time is negli-

Table 1. The χ_{zz} Element of the Polarizability Tensor $[X]$ for the Two-, Three-, Four-, and Five-Element Arrays With Varying Distance-to-Length (d/L) Ratios

	Elements in the Array			
d/L Ratio	Two	Three	Four	Five
0.1	2.084	2.796	3.449	3.887
0.25	2.403	2.523	...	...
0.5	2.468	2.918	...	...
1.0	2.641	3.780	...	...

Polarizability is in units of picofarads times square meters.

gible compared with the time required to repetitively build and solve the matrix equation repeatedly. This time-consuming feature is one of the primary disadvantages to using the frequency domain MOM approach for the computation of transients.

A second feature of using the SEM is its prediction of the peak static charge density on any general radiating system and specifically in the n-element array already presented. This provides the design engineer with an understanding of the likely attachment points of lightning. It should be noted here that even though the most probable locations for lightning strikes can be identified, in no way is this a guarantee that it will not strike some other part of the system, and therefore the entire system should be carefully investigated.

Additional applications of the SEM technique include determining the polarizability of the structure. By doing so, the general effect the structure would have on the Earth's fair weather field or other possible man-made electromagnetic quasi-static fields could be predicted (the polarizability of a structure is indicative of the direction quasi-static E-field lines would bend when in the proximity of the system). This would give the engineer practical insight into the structure's effect on local field strength measurements.

5. Conclusions

In this paper, the singularity expansion method was used to determine the electrostatic charge distribution on an n-element planar array. The results obtained using the SEM agreed well with the more conventional MOM solution of the electrostatic scalar potential equation. In addition to yielding good results, the SEM provided additional information on the system's characteristics that many previously used techniques could not.

Through numerical experimentation on planar arrays of two, three, four, and five elements, some interesting relationships among the SEM parameters were observed. On the basis of these results, some general statements concerning the SEM characteristics of an n-element array can be made. An interesting and very important SEM characteristic of the n-element array is that it has n poles in the regions where the single element has only one. These poles are system poles and related to any one particular element in the array. Furthermore, two of the n poles can be classified as either a radiation pole or a transmission line pole, depending on the direction of the corresponding modal current distributions. The remaining n-2 poles also have unique modal current distributions, but physical interpretation of the behavior of these modes becomes increasingly difficult. Moreover, the n-element array possesses all of the poles and modes of the n-2 array plus two additional distinct modes. Through an inspection of the coupling coefficients associated with these modes, only the odd harmonics of the radiation pole significantly couple into the electrostatic response. Furthermore, the fundamental radiation pole dominates this response. The higher-order modes are required to accurately represent the static charge response near the ends of the conductors.

References

Baum, C. E., On the singularity expansion method for the solution of electromagnetic interaction problems, Air Force Weapons Laboratory Interaction Notes *Note 88*, Kirtland Air Force Base, N. M., 1971.

Baum, C. E., *Transient Electromagnetic Fields*, pp. 129-179, Springer-Verlag, New York, 1976.

Boas, R. P., *Invitation to Complex Analysis*, Random House, New York, 1987.

Harrington, R. F., *Time-Harmonic Electromagnetic Fields*, McGraw-Hill, New York, 1961.

Harrington, R. F., *Field Computation by Moment Methods*, Macmillan, New York, 1968.

Pocklington, H. C., Electrical oscillations in wire, *Proc. Cambridge Philos. Soc.*, *9*, 324-332, 1897.

Riggs, L. S., Singularity expansion method (SEM) analysis of thin perfectly conducting cylindrical conductors, Ph.D. thesis, Auburn Univ., Auburn, Al, 1985.

Riggs, L. S., J. M. Lindsey, and T. S. Shumpert, Commonalities in the electrostatic characterization of several thin conducting cylinders using the singularity expansion method, *J. Electrost.*, *22*, 161-176, 1989.

Tesche, F. M., On the singularity expansion method as applied to electromagnetic scattering from thin wires, Air Force Weapons Laboratory Sensor and Simulation Notes *Note 177*, Kirtland Air Force Base, N. M., 1973.

Uman, M. A., *Lightning*, McGraw-Hill. New York, 1969.

Van Valkenburg, M. E., *Network Analysis*, Prentice-Hall, Englewood Cliffs, N. J., 1964.

M. E. Baginski, J. E. Mooney, and L. S. Riggs, Department of Electrical Engineering, 200 Broun Hall, Auburn University, Auburn, AL 36849. (e-mail: mikeb@eng.auburn.edu; mooneje@eng.auburn.edu; riggs@eng.auburn.edu)

(Received March 4, 1996; revised June 12, 1996; accepted June 21, 1996.)